INL/CON-24-76941-Revision-0

Reactor Containment Passive Safety Analysis: Steam Condensation in Presence of Non-condensable Gas Scaled Experiment and Modeling

October 2024

Changing the World's Energy Future

Palash Kumar Bhowmik, Joshua P. Schlegel

Idaho National Laboratory

INL is a U.S. Department of Energy National Laboratory operated by Battelle Energy Alliance, LLC

INL/CON-24-76941-Revision-0

Reactor Containment Passive Safety Analysis: Steam Condensation in Presence of Non-condensable Gas Scaled Experiment and Modeling

Palash Kumar Bhowmik, Joshua P. Schlegel

October 2024

Idaho National Laboratory
Idaho Falls, Idaho 83415

http://www.inl.gov

Prepared for the
U.S. Department of Energy
Under DOE Idaho Operations Office
Contract DE-AC07-05ID14517

Reactor Containment Passive Safety Analysis: Steam Condensation in Presence of Non-condensable Gas Scaled Experiment and Modeling

Palash K. Bhowmik[1,*], Joshua P. Schlegel[2], Piyush Sabharwall[1]

[1]Division of Reactor System Design and Analysis, Idaho National Laboratory, Idaho Falls, ID, USA;
[2]Department of Nuclear Engineering and Radiation Science, Missouri University of Science and Technology, Rolla, MO, USA

[leave space for DOI, which will be inserted by ANS]

ABSTRACT

This study presents steam condensation scaled experiments and semi-empirical models in presence of nitrogen (N)—a noncondensable gas (NCG), simulating air in the reactor containment—to support water-cooled small modular reactors (SMRs) passive containment cooling system (PCCS) design and analysis. Previous experimental studies on PCCS are focused on fixed and smaller tube (mostly 2-in.) geometries and specific test condition variations, bringing challenges with geometric scaling and mismatching with SMR prototypic design. To address these challenges, this study presents steam condensation test dataset obtained from three scaled test sections of 1-, 2-, and 4-in.-diameter steam condensers with an annular/jacket cooling of 2-, 3-, and 6 in.-diameter tubes, respectively. Test data were collected for steam ranges from 58 to 63 kg/hr., and NCG flow of 4.4 to 13.3 kg/hr. Annular cooling water flow was varied to obtain required testing conditions of saturated steam inlet and fully condensed outlet. Axial temperature test data of bulk cooling water, steam and condensate were collected by thermocouples for three test sections and various steam-NCG mixing/testing conditions. A standard data reduction method was adopted—utilizing iterative and nodalized mass and heat transfer calculation—to estimate axial local heat fluxes, heat transfer coefficients (HTCs), condensation rates, film thickness, and Nusselt number. Based on the obtained dataset semi-empirical model results—a ratio of experimental and Nusselt's theoretical HTC are presented. Such results and findings are supportive of developing scaled-up testing facility, to enable model validations and accelerate next generation of reactors development and deployment.

Keywords: Steam condensation, Scaled experiment, Noncondensables, Passive safety analysis, Next generation reactors

1. INTRODUCTION

Small modular reactors (SMRs) have attractive features, such as factory-built construction, modular design, easier transportation, and multi-units capacity addition [1–2]. More than 80 SMRs were in the design and development stages, and many of the reactors are water-cooled [1]. However, the verification and validation of the required models is a must for obtaining regulatory approval, which supports evaluation model development and the assessment process for the reactor system, similar to the passive containment cooling system (PCCS) for various loss-of-coolant accidents (LOCAs) [3–4]. The previous condensation heat transfer (CHT) works were grouped into theoretical, experimental, and numerical studies [5]. The

*PalashKumar.Bhowmik@inl.gov, Palash K. Bhowmik.

experimental studies were subgrouped into separate and integral effect tests with a wide range of varying geometric, physics, fluids, and operating conditions [6]. Similarly, the theoretical and numerical studies were subgrouped into conceptual modeling, simulations, and multiphysics-computational fluid dynamics (CFD) using commercial software, system, and in-house-developed codes [7]. Many of the earlier studies on the reactor in containment condensation considered the effect of non-condensable gases (NCGs), such as air, nitrogen, hydrogen, and helium [8–13].

Previous PCCS CHT experimental studies mostly focused on small and fixed geometric (mostly using a 2-in. pipe) and testing conditions causes challenges to geometric scaling and operational condition relevant to the prototypic conditions for SMRs [5–6]. Therefore, a scale test dataset and simplified modeling approach is required in most cases for early-stage reactor system design and analysis. To fill this gap, this study utilized three scaled test sections of 1-, 2-, and 4-in.-diameter steam condensers with annular/jacket cooling of 2-, 3-, and 6-in.-diameter tubes to obtain steam condensation test data (mostly axial temperature) in the presence of NCG, varying steam-NCG mix flow rates, and annular cooling flow rates. A standard data reduction method is applied to examine critical parameters, such as temperature, pressure, and steam-NCG mix distribution; local heat transfer coefficient (HTC); condensation rate; and dimensionless numbers: Reynolds number (Re) and Nusselt number (Nu), to check the scaling performance. Based on the obtained dataset semi-empirical relations, a ratio of Nusselt's theoretical HTC and experimental HTC are presented to check the effects of geometric scaling and NCG on steam condensation of the PCCS of an SMR system.

2. PHYSICS PHENOMENA AND EXPERIMENTAL APPROACH

Physics phenomena is very important for experimental data reduction method development. Figure 1(a) represents the schematics of steam condensation in presence of NCG inside the half axisymmetric condenser tube with a jacket water annular cooling and adiabatic (insulated) wall. Figure 1 also shows the schematics of the flow and temperature profile. Mixture temperatures, $T^s_\infty(z)$, and velocity, v, are the maximum at the center line, and their profiles decrease radially. The temperature at the condenser tube outer wall, the bulk coolant, and the jacket cooling tube inner wall are T_{wo}, T_b, and T_a, respectively.

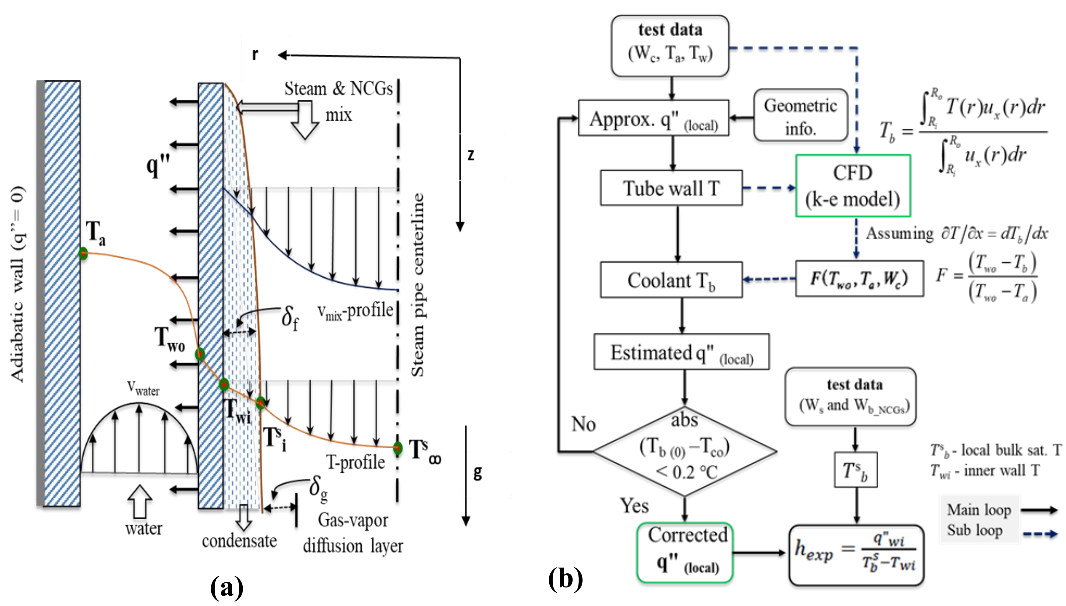

Figure 1. Schematics of CHT: (a) physical phenomena, (b) data reduction flow chart [14].

2.1. Physics Phenomena Considerations

The following physics considerations and approximations are for test data reduction method development:

- Inlet/outlet, interface flow/velocity and temperature boundary conditions. Steam-NCGs mixture enters the condensation test section at a uniform velocity, u(z) at z = 0. The inlet temperature, pressure, and gas mass fraction are T_{inlet}, P_{inlet}, and mg, respectively. At the tube wall surface, steam velocity is zero as no-slip condition or steam come in contact with the condensing tube inner wall (at T_{wi}) and cooled, condensed, and formed liquid film. The film temperature, T_f, is always below the steam saturation temperature, $T^s(z)$. The film thickness, δ, develops axially and forms downward flow.
- Heat flux, and heat transfer boundary conditions. Heat transfer from the hot mixture to the coolant occurs through the tube wall, as shown by the heat flux, q''. The condensing tube thickness, surface roughness, and material properties, such as thermal conductivity (k), affects the fluid flows and heat transfer performances. The liquid film has lower HTC, h_f, than that of pure steam, h_s, and acts as the main heat transfer resistance for pure steam condensation.
- NCG effects considerations. The NCGs cannot penetrate the liquid film; hence, it accumulates in the film and vapor interfaces. As the NCGs have a lower HTC, h_g, than that of steam, h_s, and liquid film, h_f, it reduces the interface saturation temperature, $T^s_i(z)$, and the overall HTC, h. Besides, $T^s_i(z)$ depends on interface vapor partial pressure, P_{vi}. The accumulation of the NCGs at the film-vapor interface also depends on the gas mass fraction and condensation rates.

2.2. Test Facility Description

Figure 2 presents the schematic of the test facility consisting of: (a) three different diameter test sections of condensing tubes of 1-, 2-, and 4-in., and corresponding jacket water cooling tubes/pipes of 2-, 4-, and 6-in. that are 8 ft. long and made of stainless steel 304; and (b) required piping, valves, and isolation components. Forty-four thermocouples were strategically placed to minimize measurement uncertainty to measure axial temperatures at the condensing tube wall and annular coolant. Mass flow meters measured the steam, water, and NCG mass flow rates. Thermocouples and pressure indication/measurement were used to measure the inlet/outlet pressure and temperature of the steam, water, and NCG.

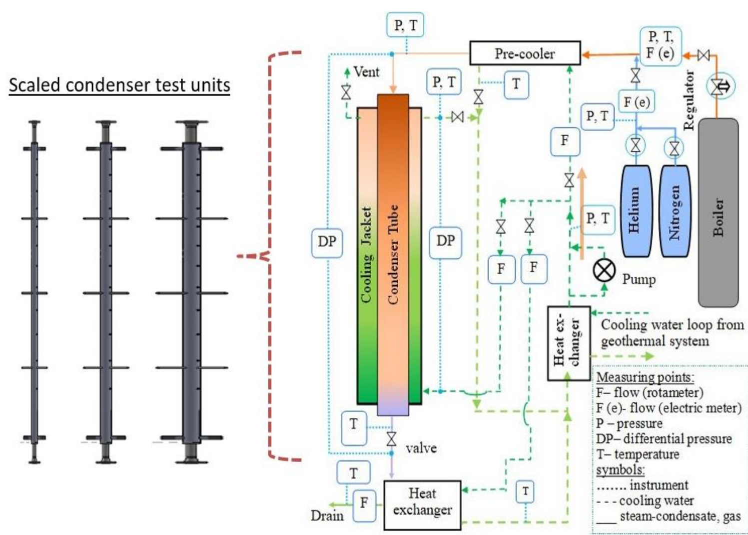

Figure 2. Final test facility instrument and control schematic [14].

2.3. Data Reduction Methodology

The test data reduction method for CHT, as outlined in Figure 1(b), consists of estimations for: (a) coolant bulk temperature (T_b) and local heat flux (q''); (b) local HTC, blowing parameter, and film thickness; (c) dimensionless parameters such as Reynolds (Re) and Nusselt (Nu) numbers; (d) uncertainty quantification; and (e) semi-empirical modeling. A data reduction method developed utilizing relevant models/equations is presented in Table I. The detailed description of the data reduction method is presented in prior experiments on pure steam condensation [14].

Table I. Data reduction method and the relevant models/equations [14].

Parameters	Models and Equations
T_b and Local q''	$$q''_{wi}(z)_{approx.} = -\frac{W_c c_p}{\pi d_i}\frac{dT_a(z)}{dz} \text{ and } T_{wi} = T_{wo} + \frac{r_i q''_{wi}(z) \ln\left(\frac{d_o}{d_i}\right)}{k_w}$$ $$q''_{wi}(z) = -\frac{W_c c_p}{\pi d_i}\frac{dT_{b,c}(z)}{dz}$$ where, $T_{b,c}$, T_{wi}, T_{wo}, and T_a, are the temperature of the coolant (bulk), condensing tube inner wall, condensing tube outer wall, and jacket water cooling. W is the mass flow rate, z is the axial length, d for diameter, k for thermal conductivity, cp for specific heat capacity; subscript c for coolant.
Local HTC, Blowing Parameter β, and Film Thickness δ	$$h_{exp} = \frac{q''_{wi}}{T_b^S - T_{wi}}, \text{ and } \Gamma = \frac{g}{\mu}\rho_1(\rho_1 - \rho_m)\frac{\delta_f^3}{3} + \frac{\rho_1 \tau_i \delta_f^2}{2\mu_1}$$ $$\tau_i = 0.5 f_{io} \rho_m (u_m - u_i)^2 \frac{\beta_f}{\exp(\beta_f) - 1}$$ $$\beta_f = \frac{m''}{\rho_m u_m f_{io}/2} \text{ and } \delta_{fo} = \left(\frac{3u_1\Gamma}{g\rho_1(\rho_1 - \rho_m)}\right)^{1/3}$$ where, h for HTC, δ for film thickness, Γ for liquid flow per unit perimeter, g for gravity, μ for dynamic viscosity [kg/m s], τ interfacial shear stress; and subscript i and l for inner/interface and liquid, respectively.
Dimensionless Numbers: Re and Nu	$$\frac{Re_f}{1 - \left(\frac{\rho_m}{\rho_1}\right)} = \frac{\delta_f^{*3}}{3} + \frac{\tau_i^* \delta_f^{*2}}{2}; \; Nu_f = \frac{h_f L}{k_c} = \left(Nu_{f,h}^4 + Nu_{f,tu}^4\right)^{1/4}$$ $$Nu_{f,la} = \frac{1}{\delta_f^*} \text{ and } Nu_{f,tu} = aRe_f^b \, Pr^c \left(1 + e\tau_i^{*f}\right)$$ where, Re for Reynolds number, Nu for Nusselt number, Pr for Prandtl number, and L for characteristics length. Subscript f for film, m for mix, i for interface, tu for turbulent.
Degradation Factor, (DF, f)	$f = \frac{h_{exp}(z)}{h_{Nu}(z)}$, where, experimental HTC, $h_{exp}(z)$ and Nusselt's HTC, $h_{Nu}(z)$.
Uncertainty Quantification	$$\frac{\sigma_{exp}}{h_{exp}} = \left[\left(\frac{\sigma_{W_{cw}}}{W_{cw}}\right)^2 + \left(\frac{\sigma_{c_p}}{c_p}\right)^2 + \left(\frac{\sigma_{d_i}}{d_i}\right)^2 + \left(\frac{\sigma_{(T_c - T_w)}}{(T_{sat} - T_{wi})}\right)^2 + \left(\frac{\sigma_{(cw/dx)}}{dT_{cw}/dx}\right)^2\right]^{1/2}$$ where, σ for error, dx for axial node length. Subscript sat for saturation, exp for experiment.

2.4. Semi-empirical Modeling

The test data were used to develop the semi-empirical correlations (i.e., the degradation factor [DF or f]), which was the ratio of the experimental and Nusselt's HTC that was first proposed by Vierow (1990) [15], and then developed by Kuhn et al. (1996) [16], Park and No (1999) [17], and Lee and Kim (2008) [18], as presented in Table II. This study uses a simplified DF relationship that represents DF for scaled geometries for steam-NCG (N_2) test dataset.

Table II. Semi-empirical models/equations [6].

Parameters	Semi-empirical Models/Correlations
Vierow (1990) [15]	$$f = \frac{h_{\exp}}{h_{Nu}} = f_1 \cdot f_2 = \left(1 + \mathrm{aRe}_{\mathrm{mix}}^{\mathrm{d}}\right) \cdot \left(1 - \mathrm{bM}_{\mathrm{NCGs}}^{\mathrm{c}}\right)$$ where, f with f_1, including the effect of interfacial shear (δ_{shear}) and surface waviness to improve the film heat transfer.
Kuhn et al. (1996)[16]	$$f = \frac{h_{\exp}}{\mathrm{h_{Nu}}} = \frac{\delta_{\mathrm{shear}}}{\delta_{\mathrm{Nu}}} \cdot \left(1 + \mathrm{a}\left(\frac{\mathrm{Re_f}}{4}\right)^{\mathrm{d}}\right) \cdot \left(1 - \mathrm{bM}_{\mathrm{NCGs}}^{\mathrm{c}}\right)$$ This is the modified Vierow (1990) f with f_1, including the effect of interfacial shear (δ_{shear}) and surface waviness. The details parameter information of f is available in Table 2 of Bhowmik et al. (2022) [6].
Park and No (1999) [17]	$$f = \frac{\mathrm{h_{tot}}}{\mathrm{h}_f} = 0.0012\ \mathrm{W_{nc}^{-1.4} Ja^{-0.63} Re_f^{0.24}}$$ for $1715 < \mathrm{Re_g} < 21670, 0.83 < \mathrm{Pr_g} < 1.04, 0.111 < \mathrm{M_{air}} < 0.836$, $0.01654 < \mathrm{Ja} < 0.07351$, and $12.4 < \mathrm{Re_f} < 633.6$. where, dependence of steam-NCGs mixture Re and Prandtl number, Pr on CHT and developed f using gas mass fraction, Jacob number, Ja and liquid film Re.
Lee and Kim (2008) [18]	$$f = \tau_{\mathrm{g}}^{*0.3124}\left(1 - 0.964\mathrm{M_a^{0.402}}\right)$$ for $0.06 < \tau_g^* < 46.65, 0.038 < M_{\mathrm{air}} < 0.814$ where, f for steam-NCGs mixture in a U-tube in a reflux condensation, using gas mass fraction and shear force of the mixture.

3. RESULTS AND DISCUSSION

Test data were collected for varying steam-NCG mixture mass fractions (M, %), steam-NCG mass flow rates, and coolant flow rates, as presented in Table 3. Figure 3, Figure 4, and Figure 5, respectively, present representative sample test datasets for the 4-in. test section, which were collected under a wide range of NCG mass flow rates (e.g., high, moderate, and low). Tests A-run0.9N0a, A-run2.1N4, and A-run2.1N8 represent the high (i.e., 13.22 kg/hr), moderate (i.e., 8.08 kg/h), and low (i.e., 4.41 kg/h) NCG:N_2 flow cases, respectively. These selected test cases and levels were intended to enable a qualitative comparison of all N_2 test cases, but the cases were not applicable to all test datasets. The selected tests were conducted under saturated steam conditions at approximately atmospheric pressure (e.g., 100–128 kPa) with ambient discharge. A simple degradation factor using semi-empirical (i.e., ratio of experimental HTC, to Nusselt's HTC) evidence represents the scaled steam-NCG test data, as shown in Figure 6.

Table III. Selected steam-N2 mix condensation test conditions/ranges.

Test Section	Steam flow	Pin	Tin	NCF: N_2 flow	M
1-in	30-53	109.6-109.9	100.2-103	2.9-14.7	5.5-23.6%
2-in	30.7-42.2	111.4-115.7	102.6-105.4	2.6-12.9	6.1-31.6%
4-in	54.7-60.1	140.4-150.4	99.4-103.5	4.4-3.2	7-18.1%

Note: Here, TS for test section, inlet mass flow rate (F [kg/hr)] for steam and NCG[N], inlet pressure (Pin [kPa]), inlet temperature (Tin [∘ C]), and NCG mass fraction (M, %).

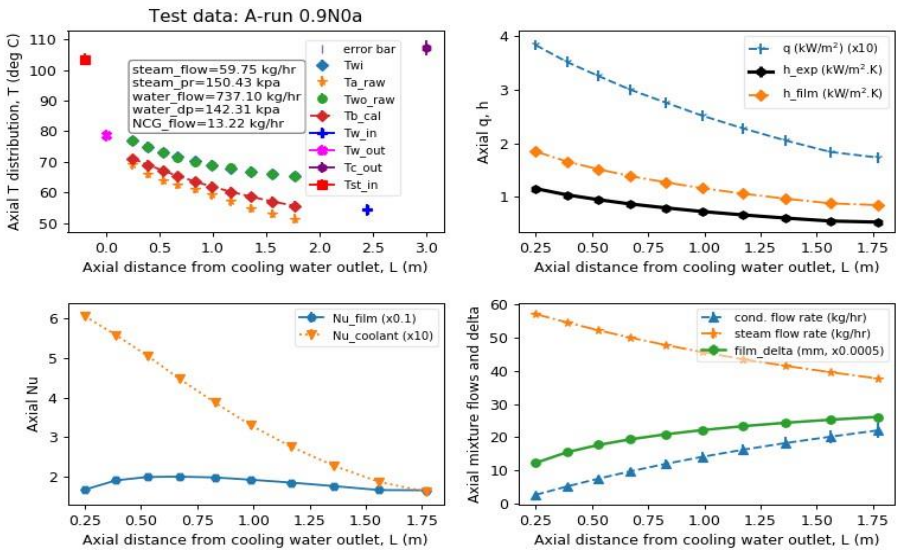

Figure 3. Test data: A-run0.9N0a (4-in. test section; NCG: N_2, high flow).

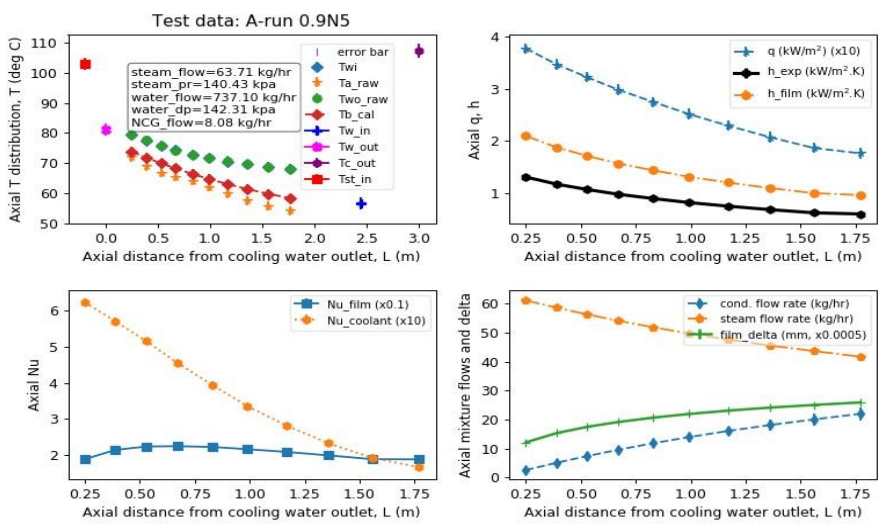

Figure 4. Test data: A-run0.9N5 (4-in. test section; NCG: N_2, medium flow).

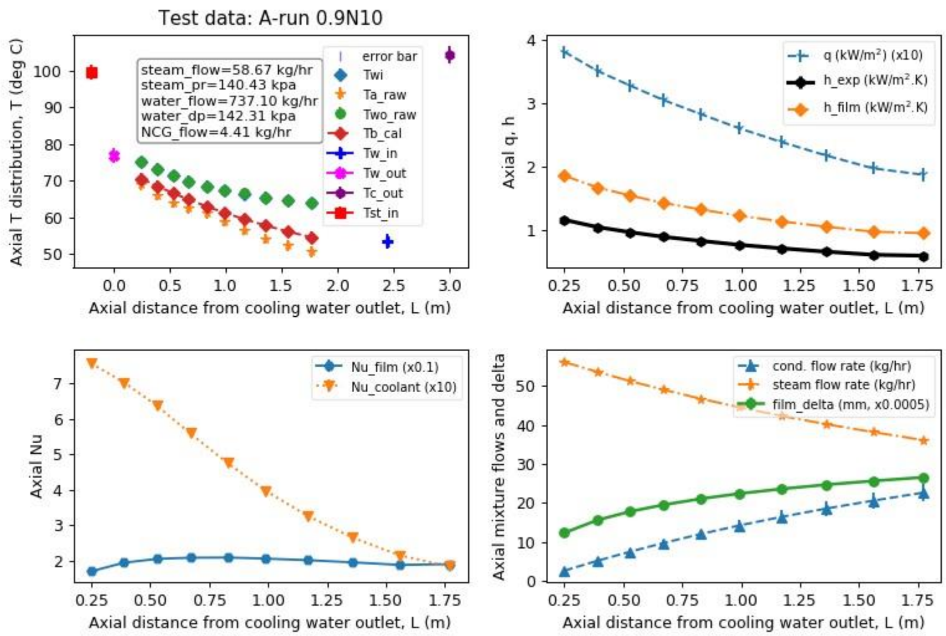

Figure 5. Test data: A-run0.9N10 (4-in. test section; NCG: N_2, low flow).

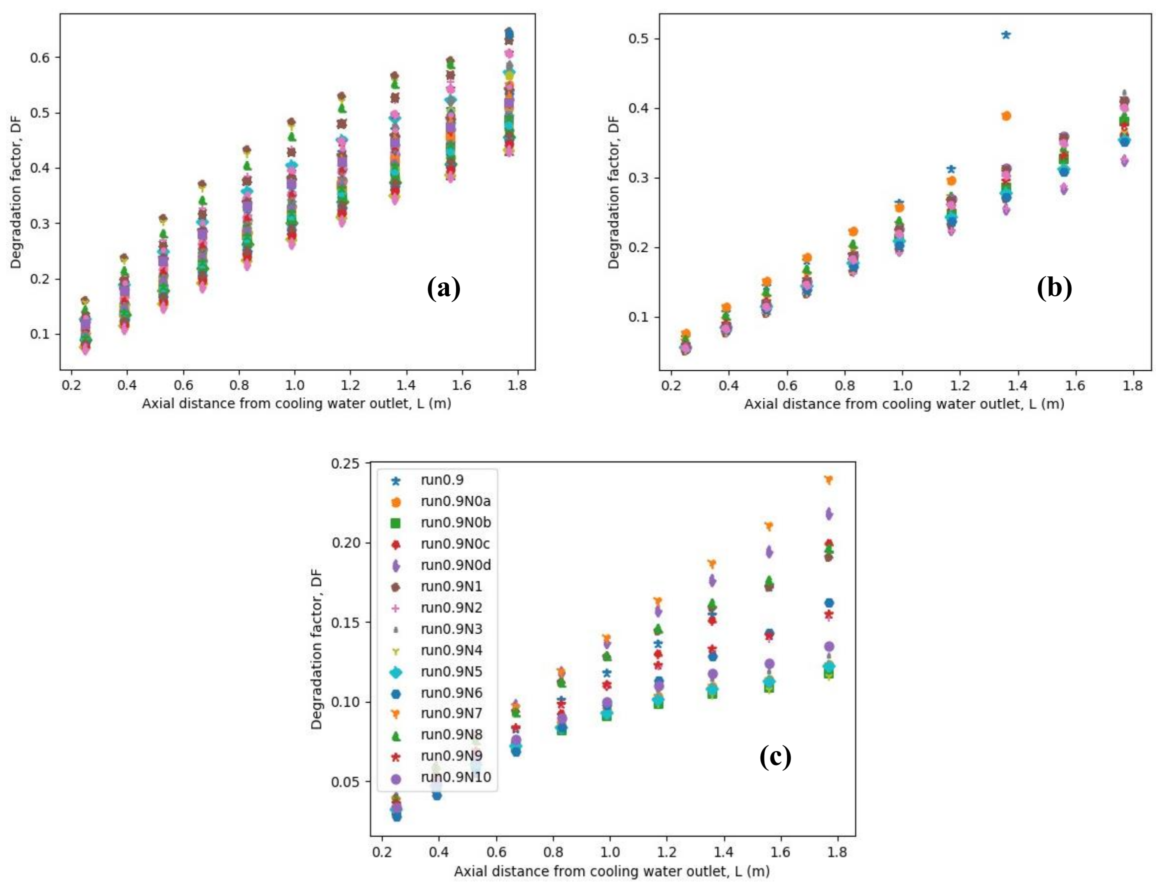

Figure 6. DF for steam-N_2 test cases: (a) 1-in., (b) 2-in., and (c) 4-in. test sections.

The following observations resulted from the experiments and test data analysis:

- Test data showed the CHT, HTC, and condensation rate all decreased with an increase in NCGs. In contrast, these values increased as the steam mass flow increased. The test data were collected at a certain distance from the inlet and outlet to avoid entrance and exit effects.
- A series of similar tests was conducted for varying steam mass flow rates, pressures, and NCG mass fractions. Test data showed qualitative consistency. However, better consistency of the test data would be achievable by introducing adequate control elements (e.g., control valves) to control the testing conditions (e.g., steam-NCG mix inlet mass flow rates, temperature, and pressure), as well as controlling the cooling and condensate discharge.
- The estimated DF, as shown in Figure 6, for the various test sections and steam-nitrogen tests exhibited that with an increase in the diameter of the condenser tube, the DF decreased and ranged from 0.1 to 0.7, 0.05 to 0.4, and 0.05 to 0.25 for the 1-in., 2-in., and 4-in. test geometries, respectively. Note that there are a few inconsistent data points for the 2-in. tests, which are outliers. This test dataset could improve verification and validation efforts of computation models and tools [19, 20], which will further improve understanding of the detailed thermal-hydraulics behavior.

4. CONCLUSIONS

To analyze the physical phenomena behind SMR PCCSs, this study presents scaled experiments regarding steam condensation in the presence of NCGs. The tests involved vertical downward steam flow and condensation within the inner surfaces of condenser tubes, coupled with annular or pool-cooling methods. Test data were collected for various steam and NCG flow rates, as well as temperature/pressure conditions. Accidents involving steam release to the reactor containment varies for various LOCA scenarios (e.g., main steam line break, steam generator tube ruptures) and accident phases. Steam condenses on the containment walls by releasing heat, while condensates accumulate in the containment sump. A few observations and conclusions can be derived from this study:

- This study focused on later-stage accident phases—mostly long-term cooling—for standard SMRs, which occur about 72 hours into the cooling period following an initiation of an accident and utilized three different scaled geometry test sections.
- Steam condensation considered in the study comprised of film-wise and dropwise; however, for dominating steam condensation in reactor containment during long-term cooling, this study focused on the film-wise type in which a liquid film covers the containment surface.
- Figures of merit for the reactor system steam release accident to reactor containment are mainly containment pressure and temperature, which are the primary test parameters for this study.
- This study presents scaled test data and results for steam condensation in the presence of nitrogen, which simulates air for the containment system. The percentage of air presence in steam release accidents varies over the accident phases. As this study focuses on long-term cooling and film condensation, the physics approximation of NCGs is considered as a barrier to bulk steam for film heat transfer, which is related to NCG partial pressure—an important phenomenon of interest.
- Simple semi-empirical representation of the test data using the degradation factor provides a general relation with experimental and theoretical HTC estimation, including the effect of NCG.
- Future research could encompass validating steam condensation CFD and system code models, and obtaining qualified data, which would identify scaling factors, scaling distortion, and uncertainty associated with geometric and testing conditions, for decision-making to develop qualified test facilities at prototypic conditions.

In summary, understanding the PCCS design for a specific reactor system, identifying the phenomena of interest, and specifying the figures of merit, especially during the long-term cooling, is essential for reactor system design, analysis, and regulatory approvals. In addition, improvement in the scaled-value empirical correlations and integrated multiphysics-system code modeling would certainly improve the design and analysis and enable accelerated deployment for next generation reactors.

NOMENCLATURE

CFD	Computational fluid dynamics
CHT	Condensation heat transfer
DF	Degradation Factor
HTC	Heat Transfer Coefficient
LOCA	Loss-of-coolant accident
NCG	Noncondesable Gas
PCCS	Passive Containment Cooling System
SMR	Small Modular Reactor

ACKNOWLEDGMENTS

The authors thank the Small Modular Reactor Research and Education Consortium and Department of Mining and Nuclear Engineering at Missouri University of Science and Technology for the research support; and Irradiation Experiment and Thermal Hydraulics Analysis Department at Idaho National Laboratory (INL) for professional development and support.

Conflicts of Interest: The authors declare no conflict of interest.

REFERENCES

1. IAEA, 2022. “Small Modular Reactors: A new nuclear energy paradigm, pre-print,” International Atomic Energy Agency (IAEA), Vienna, Austria (2022).
2. Schlegel, J. P., and P. K. Bhowmik, 2024. “Chapter 14 - Small modular reactors,” In: Editor(s): Jun Wang, Sola Talabi, and Sama Bilbao y Leon, *Nuclear Power Reactor Designs*, Academic Press, San Diego, CA, USA. Pages 283–308. https://doi.org/10.1016/B978-0-323-99880-2.00014-X.
3. U.S. NRC Regulatory Guide 1.203. 2005 [cited 8 January 2024]. Available from: https://www.nrc.gov/docs/ML0535/ML053500170.pdf (accessed 2 February 2024).
4. Bhowmik, P. K., C. E. E. Perez, J. D. Fishler, S. A. B. Prieto, I. D. Reichow, J. T. Johnson, P. Sabharwall, and J. E. O'Brien, 2023. “Integral and separate effects test facilities to support water cooled small modular reactors: A review.” *Prog. Nucl. Energy*, 160, 104697. https://doi.org/10.1016/j.pnucene.2023.104697.
5. Yadav, M. K., S. Khandekar, and P. K. Sharma, 2016. “An integrated approach to steam condensation studies inside reactor containments: A review,” *Nucl. Eng. Des.*, 300, 181–209. https://doi.org/10.1016/j.nucengdes.2016.01.004.
6. Bhowmik, P. K., J. P. Schlegel, and S. Revankar, 2022. “State-of-the-art and review of condensation heat transfer for small modular reactor passive safety: Experimental studies,” *Int. J. Heat Mass Transf.*, 192, 122936. https://doi.org/10.1016/j.ijheatmasstransfer.2022.122936.

7. Bhowmik, P. K., J. P. Schlegel, and S. Revankar, 2023. "State-of-the-art and review of condensation heat transfer for small modular reactor passive safety: Computational studies," *Nucl. Eng. Des.*, 410, 112366. https://doi.org/10.1016/j.ijheatmasstransfer.2022.122936.

8. Bhowmik, P. K., and J. P. Schlegel, 2023. "Multicomponent gas mixture parametric CFD study of condensation heat transfer in small modular reactor system safety," *Exp. Comput. Multiph. Flow*, 2023. 5(1), 15–28. https://doi.org/10.1007/s42757-022-0136-8.

9. Lee, K. Y., 2007. "The Effects of Noncondensable Gas on Steam Condensation in a Vertical Tube of Passive Residual Heat Removal System," Ph.D. thesis, Department of Mechanical Engineering, Pohang University of Science and Technology, Pohang, Korea.

10. Solanki, D. K., N. Dhileeban, R. S. Rao, A. K. Deo, P. K. Baburajan, A. Sridharan, and S. V. Prabhu, 2023. "Steam condensation on a circular tube in the presence of non-condensables (air) in passive containment cooling system," *Int. J. Heat Mass Transf.*, 213, 124323. https://doi.org/10.1016/j.ijheatmasstransfer.2023.124323.

11. Bae, B.-U., S. Kim, Y.-S. Park, and K.-H. Kang, 2020. "Experimental investigation on condensation heat transfer for bundle tube heat exchanger of the PCCS (passive containment cooling system)," *Ann. Nucl. Energy*, 139, 107285. https://doi.org/10.1016/j.anucene.2019.107285.

12. Haag, M., P. K. Selvam, and S. Leyer, 2020. "Effect of condenser tube inclination on the flow dynamics and instabilities in a passive containment cooling system (PCCS) for nuclear safety," *Nucl. Eng. Des.*, 367, 110780. https://doi.org/10.1016/j.nucengdes.2020.110780.

13. Chen, R., P. Zhang, P. Ma, B. Tan, Z. Wang, D. Zhang, w. Tian, S. Qiu, and G. H. Su, 2020. "Experimental investigation of steam-air condensation on containment vessel," *Ann. Nucl. Energy*, 136, 107030. https://doi.org/10.1016/j.anucene.2019.107030.

14. Bhowmik, P. K., S. Usman, and J. P. Schlegel, 2023. "Film condensation with high heat fluxes and scaled experiments using pure steam for reactor containment cooling," *Appl. Therm. Eng.*, 229, 120610. https://doi.org/10.1016/j.applthermaleng.2023.120610.

15. Vierow, K. M., 1990. "Behavior of steam-air systems condensing in cocurrent vertical downflow," MS Thesis, University of California—Berkeley, Berkeley, CA, USA.

16. Kuhn, S., P. Peterson, and V. Schrock, 1996. "Determination of the local heat flux in condensation experiments," *Exp. Heat Transf.*, 9(2), 149–163. https://doi.org/10.1080/08916159608946519.

17. Park, H. S., and H. C. No, 1999. "A condensation experiment in the presence of noncondensables in a vertical tube of a passive containment cooling system and its assessment with RELAP5/MOD3.2." *Nucl. Technol.*, 127(2), 160–169. https://doi.org/10.13182/NT99-A2992.

18. Lee, K. Y., and M. H. Kim, 2008. "Experimental and empirical study of steam condensation heat transfer with a noncondensable gas in a small-diameter vertical tube," *Nucl. Eng. Des.*, 238(1), 207–216. https://doi.org/10.1016/j.nucengdes.2007.07.001.

19. Bhowmik, P.K., Schlegel, J.P., Kalra, V. Alam, S. B., Hong, S., & Usman, S. (2022). CFD validation of condensation heat transfer in scaled-down small modular reactor applications, Part 2: Steam and non-condensable gas. *Exp. Comput. Multiph. Flow* 4, 424–434 (2022). https://doi.org/10.1007/s42757-021-0113-7

20. Bhowmik, P.K., Schlegel, J.P., Kalra, V. Alam, S. B., Hong, S., & Usman, S. (2022). CFD validation of condensation heat transfer in scaled-down small modular reactor applications, Part 2: Steam and non-condensable gas. *Exp. Comput. Multiph. Flow* 4, 424–434 (2022). https://doi.org/10.1007/s42757-021-0113-7